Structure of the A, B, and C Absorption Bands in KCl : Tl

A. M. Lemos, M. C. Stauber,* and J. F. Marion
Adelphi University, Garden City, New York 11530
(Received 24 June 1970)

A twelvefold dengenerate perturbation technique is used to determine wave functions and eigenenergies of the first excited state of Tl^+ in an O_h field. The governing Hamiltonian includes exchange, spin-orbit, static O_h, and dynamic electron-lattice interactions. This dynamic interaction is approximated by a term linear in the lattice coordinates. The resulting 12×12 interaction matrix is numerically diagonalized, yielding eigenfunctions and eigenenergies as functions of lattice coordinates. These results are used to determine transition probabilities and oscillator strengths for transitions from the $6s^2$ ground state to the $6s6p$ excited state. The main conclusions reached are (a) the A, B, and C bands are composed of subsidiary temperature-dependent bands. The A band is a doublet at low temperature and a triplet at higher (300°K) temperatures. The C band is a triplet at all temperatures, and the B band is a strongly temperature-dependent doublet. (b) The C- and A-band oscillator strengths are almost constant over a wide range of temperature. However, the C-band oscillator strength decreases at very high temperatures. (c) The B-band oscillator strength is a rapidly increasing function of temperature, and its shape is *not* Gaussian or near-Gaussian at higher temperature. (d) No transitions occur from the ground state to the $^2P_0$ (i.e., $|{}^3A_1u\rangle$) state.

INTRODUCTION

When heavy-metal ions such as Tl^+, Pb^{++}, In^+, etc., are substitutionally deposited in alkali-halide crystals, new absorption and emission bands appear. These bands are directly attributable to the presence of the impurity ion.[1] The purpose of this paper is to examine the structure of the A, B, and C absorption bands associated with the Tl^+ impurity ion. In KCl:Tl, measured at liquid-nitrogen temperatures, these bands appear at 5.03, 5.94, and 6.30 eV, respectively. It is assumed that the bands are due to phonon-broadened bound-state electron transitions. These transitions proceed from the nondegenerate $6s^2$ ground state to the twelvefold degenerate $6s6p$ excited state of the trapped ion. In the free ion, the states associated with these configurations are the $^1S_0$ ground state and the spin-orbit split triplet $^3P_{2,1,0}$ and singlet $^1P_1$ excited states. Only the $^1S_0 \rightarrow {}^1P_1$, and the $^1S_0 \rightarrow {}^3P_1$ spin-orbit allowed transitions are observed in the free ion. In the crystal, these are assigned to the most intense C band and the less intense A band. The least intense B band is assigned to the $^1S_0 \rightarrow {}^3P_2$ transition which is induced via electron-phonon interactions.[2]

In addition to giving rise to the B band, this interaction accounts for the observed temperature-dependent structure of the bands.[3-5] The structure is due to the new transitions which occur as a result of lifting the degeneracy of the excited state. Thus, in order to investigate the band structure, we have made a twelvefold degenerate perturbation calculation on the excited state. The resulting wave functions are then used to calculate both transition probabilities and oscillator strengths. Our results indicate that (a) the C and A bands are composed of three temperature-dependent subbands, (b) the B band is composed of two strongly temperature-dependent subbands, (c) the C- and A-band oscillator strengths are almost constant, and (d) the B-band oscillator strength increases almost exponentially with temperature. The theoretical results agree very well with recent experimental work done at Brookhaven National Laboratory.[5]

WAVE FUNCTIONS AND SYMMETRY CONSIDERATIONS

When a heavy-metal ion such as Tl^+ is substitutionally deposited in an alkali-halide crystal it occupies an "on-site" position and is thus subjected to a field possessing O_h symmetry. The two-electron Hamiltonian (two valence electrons), including spin-orbit, electron-electron, and electron-lattice interactions, is

$$H=\sum_{i=1}^{2}\left[-\frac{\hbar^2}{2m}\nabla_i^2+\frac{z'e^2}{r_i}+\xi_i(r)\vec{l}_i\cdot\vec{s}_i\right]+\frac{e^2}{r_{12}}+V(\vec{r},\vec{R})\,. \tag{1}$$

A first-order expansion of the electron-lattice interaction $V(\vec{r},\vec{R})$ about the equilibrium configuration of the lattice, $\vec{R}_0$, yields

$$V(\vec{r},\vec{R})=V(\vec{r},\vec{R}_0)+\sum_i\left(\frac{\partial V}{\partial R_i}\right)_{R_{i0}}(R_i-R_{i0})\,. \tag{2}$$

Here $\vec{r}$ refers to electron coordinates and $\vec{R}$ to ion coordinates. The first term in the expansion is the electrostatic O_h interaction and the second term is the linear or dynamic Jahn-Teller interaction.[6]

Static Interaction

As mentioned above, the $6s^2$ ground state is nondegenerate and the $6s6p$ excited state is twelvefold

degenerate in the quantum number M_J. The spin-orbit and exchange interactions partially split this degeneracy into four separate levels which correspond to the familiar $^1P_1$, $^3P_2$, $^3P_1$, and $^3P_0$ states. The only allowed transitions are the $^1S_0 \rightarrow {}^1P_1$ which corresponds to the C band and the spin-orbit allowed $^1S_0 \rightarrow {}^3P_1$ which corresponds to the A band. The effect of the static O_h interaction $V(\vec{r}, \vec{R}_0)$ is to shift the levels and to partially lift the degeneracy of the $^3P_2$ state. However, this static interaction does not give rise to any new $6s^2 \rightarrow 6s6p$ transitions.

The wave functions for the ion in the crystal are constructed by combining the free-ion functions in such a way that they transform like the basis functions for the irreducible representations of the O_h group. In this way they will be eigenfunctions of a Hamiltonian which is invariant under the operations of the O_h group. The irreducible representations corresponding to the free-ion states are $^1T_{1u} \rightarrow {}^1P_1$, $^3E_u + {}^3T_{2u} \rightarrow {}^3P_2$, $^3T_{1u} \rightarrow {}^3P_1$, $^3A_{1u} \rightarrow {}^3P_0$, $^1A_{1g} \rightarrow {}^1S_0$. These basis functions are derived in Ref. 7 and listed in Ref. 8.

The effect of the spin-orbit interaction is to mix the $|\,^1T_{1u}\rangle$ and $|\,^3T_{1u}\rangle$ states. The resulting mixed states are

$$|C\rangle_i = (1-t^2)^{1/2}\,|\,^1T_{1u}\rangle_i + t\,|\,^3T_{1u}\rangle_i \tag{3a}$$

and

$$|A\rangle_i = -t\,|\,^1T_{1u}\rangle_i + (1-t^2)^{1/2}\,|\,^3T_{1u}\rangle_i \ . \tag{3b}$$

Here the subscript i refers to the three states corresponding to $M_j = 1, 0, -1$. t is the spin-orbit coupling constant which is determined by the King–van Vleck (KV) procedure.[9] To this point, the wave functions are eigenfunctions of the Hamiltonian which includes exchange (accounted for in the KV procedure), spin-orbit, and static O_h interactions. These wave functions are $|C\rangle_i$, $|A\rangle_i$, $|\,^3E_u\rangle_j$, $|\,^3T_{2u}\rangle_i$, $|\,^3A_{1u}\rangle$, and $|\,^1A_{1g}\rangle$, where the $|T\rangle$ states are triply degenerate ($i = 1, 2, 3$), the $|E\rangle$ state doubly degenerate ($j = 1, 2$), and the $|A_{g,u}\rangle$ states nondegenerate. The primary orbital form of these states is shown in Fig. 1. It should be noted that the only states which can be reached by a dipole transition from the ground state are the $|C\rangle_i$ and the $|A\rangle_i$ states which correspond to the A and C bands.

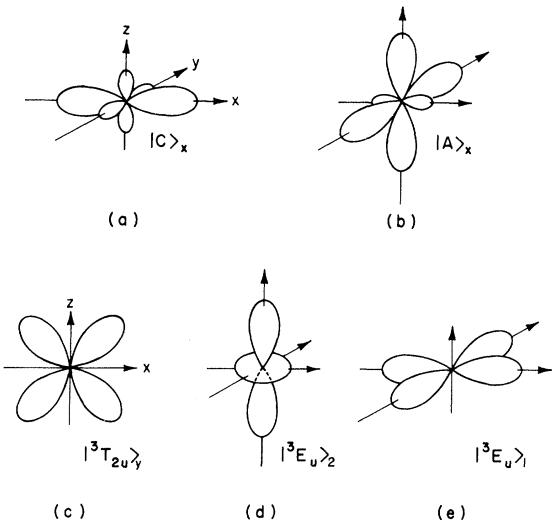

FIG. 1. Orbital forms for the $6s6p$ basis functions in an O_h field.

Dynamic Interaction

Consider now the linear electron-lattice interaction described in Eq. (2). In a normal-coordinate representation this becomes $\sum_j \gamma_j Q_j$, where γ_j, the electron-lattice coupling coefficient for interaction with the jth vibrational mode of the lattice, is a function of electron coordinates. Using the tight-binding approximation, we assume that the vibronic modes which dominate the electron-lattice interaction are localized about the Tl^+ ion. In essence, an octohedral XY_6 molecule is taken as the model for the Tl^+ ion in a vibrating O_h environment. The normal modes for such a molecule have the symmetries of the irreducible representations of the O_h group. The group-theory designations for these modes are A_{1g}, E_g, T_{1u}, T_{2u}, and T_{2g}.[10]

In determining the wave functions and the eigenvalue splitting of the degenerate state, we have used the following technique. The Hamiltonian, Eq. (1), is rewritten as

$$H = H_0 + H' \ , \tag{4}$$

where

$$H' = e^2/r_{12} + \sum_{i=1}^{2} \xi(\vec{r})\vec{l}_i \cdot \vec{s}_i + V(\vec{r}, \vec{Q}_0) + \sum_i \gamma_i Q_i \ . \tag{5}$$

H_0 is treated as the unperturbed Hamiltonian and H' as the perturbation which lifts the degeneracy of the first excited state. The basis functions for the perturbation expansion are the eigenfunctions described above as $|C\rangle_i$, $|A\rangle_i$, etc. The approach has been used by Kamimura and Sugano[11] and recently by Honma,[12] and in light of our computer program, proves to be very convenient. Since the expansion covers twelve states, the perturbation matrix to be diagonalized is 12×12. Because of the choice of basis functions, however, all off-diagonal elements are due to the linear interaction. Furthermore, since the excited state has odd parity ($L = 1$), only even-parity modes will contribute to the perturbation matrix. These even-parity modes are illustrated in Fig. 2.

Interaction Matrix

The resulting Hermitian matrix is shown in Fig. 3. The terms E_c, E_{b1}, etc., which appear along the major diagonal, are the eigenenergies of the states $|C\rangle_i$, $|\,^3E_u\rangle$, etc. We have associated the $|C\rangle_i$ states

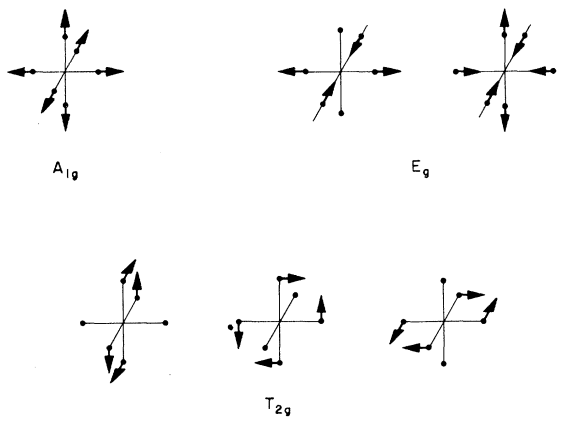

FIG. 2. Even-parity vibrational modes.

with the C band, the $|{}^3E_u$ and $|{}^3T_{2u}\rangle$ states with the B band, and $|A\rangle_i$ states with the A band. The energy are taken to be the experimental peak energies of the respective bands. The two values E_{b1} and E_{b2} arise from the static O_h splitting of the ${}^3P_2$ level previously discussed.[7,13] E_x, the value associated with the $|{}^3A_{1u}\rangle$ state, was estimated by comparing the known free-ion levels with the associated levels in the crystal. In the actual computer calculation, $E_{b1} - E_{b2}$ was varied from 0.0 to 0.2 eV (the half-width of the band) and E_x was varied by about 25%. The results proved to be almost completely insensitive to such variations. The constants b and c, which appear in the matrix, are simply the tetragonal (E_g) and the trigonal (T_{2g}) coupling constants. For a thorough discussion of these constants, the reader should refer to Refs. 8 and 14. Actually, another coupling constant related to the breathing mode (A_{1g}) should appear. However, since this term appears equally in each diagonal element, its effect has been absorbed in the energy eigenvalues. In the actual diagonalization, which was accomplished numerically using the Jacobi technique, a fixed set of values was chosen for the energy terms. The values of b and c were taken from Ref. 8. The diagonalization was then carried out for sets of points in the five-dimensional (Q_2, Q_3, Q_4, Q_5, Q_6) "Q space." Since this space was covered, it is clear that the general results cannot be very sensitive to the particular choice of b and c. The results of the diagonalization yielded a set of twelve eigenvalues and associated twelve-dimensional eigenvectors for each point in the "Q space."

TRANSITION PROBABILITIES

A subsidiary program was included in the main program which yielded both corresponding transition probability and oscillator strengths for each new state at each point. In this way, it was possible to follow the energy shifts and the transition probability of any given state in the Q space. The matrix element which determines transition probabilities is $\langle \Psi_f | \vec{r} | A_{1g} \rangle$. A_{1g} is the ground state, Ψ_f is a final-state superposition of the 12 basis states described above, and $\vec{r} = \vec{r}_1 + \vec{r}_2$, $\vec{r}_1$ and $\vec{r}_2$ being position vectors of the two valence electrons. It should be noted that the only contributing final-state component is the pure $|{}^1T_{1u}\rangle_i$ which corresponds to the

	C_x	C_y	C_z	${}^3T_{2ux}$	${}^3T_{2uy}$	${}^3T_{2uz}$	${}^3E_{u1}$	${}^3E_{u2}$	A_x	A_y	A_z	${}^3A_{1u}$
C_x	$E_C + GbQ_{t_1}$	GcQ_6	GcQ_5	$-\frac{tb}{2}Q_{t_3}$	$\frac{tc}{2}Q_6$	$-\frac{tc}{2}Q_5$	$\frac{tc}{2}Q_4$	$\frac{\sqrt{3}}{2}tcQ_4$	DbQ_{t_1}	DcQ_6	DcQ_5	0
C_y		$E_C - GbQ_{t_2}$	GcQ_4	$-\frac{tc}{2}Q_6$	$-\frac{tb}{2}Q_{t_4}$	$\frac{tc}{2}Q_4$	$\frac{tc}{2}Q_5$	$\frac{\sqrt{3}}{2}tcQ_5$	DcQ_6	$-DbQ_{t_2}$	DcQ_4	0
C_z			$E_C + \frac{2}{\sqrt{3}}GbQ_3$	$\frac{tc}{2}Q_5$	$-\frac{tc}{2}Q_4$	tbQ_2	$-tcQ_6$	0	DcQ_5	DcQ_4	$\frac{2}{\sqrt{3}}DbQ_3$	0
${}^3T_{2ux}$				$E_{b_1} - \frac{b}{2}Q_{t_1}$	$\frac{c}{2}Q_6$	$\frac{c}{2}Q_5$	$-\frac{c}{2}Q_4$	$\frac{c}{\sqrt{12}}Q_4$	$\frac{Fb}{2}Q_{t_3}$	$\frac{Fc}{2}Q_6$	$-\frac{Fc}{2}Q_5$	$\sqrt{\frac{2}{3}}cQ_4$
${}^3T_{2uy}$					$E_{b_1} + \frac{b}{2}Q_{t_2}$	$\frac{c}{2}Q_4$	$\frac{c}{2}Q_5$	$\frac{c}{\sqrt{12}}Q_5$	$-\frac{Fc}{2}Q_6$	$\frac{Fb}{2}Q_{t_3}$	$\frac{Fc}{2}Q_4$	$\sqrt{\frac{2}{3}}cQ_5$
${}^3T_{2uz}$						$E_{b_1} - \frac{b}{\sqrt{3}}Q_3$	0	$-\frac{c}{\sqrt{3}}Q_6$	$\frac{Fc}{2}Q_5$	$-\frac{Fc}{2}Q_4$	$-FbQ_2$	$\sqrt{\frac{2}{3}}cQ_6$
${}^3E_{u1}$							$E_{b_2} - \frac{b}{\sqrt{3}}Q_3$	$-\frac{b}{\sqrt{3}}Q_2$	$-\frac{Fc}{2}Q_4$	$-\frac{Fc}{2}Q_5$	FcQ_6	$\sqrt{\frac{2}{3}}bQ_2$
${}^3E_{u2}$								$E_{b_2} + \frac{b}{\sqrt{3}}Q_3$	$-\frac{\sqrt{3}}{2}FcQ_6$	$-\frac{\sqrt{3}}{2}FcQ_5$	0	$\sqrt{\frac{2}{3}}bQ_3$
A_x									$E_A + HbQ_{t_1}$	HcQ_6	HcQ_5	0
A_y										$E_A - HbQ_{t_2}$	HcQ_4	0
A_z											$E_A + \frac{2}{\sqrt{3}}HbQ_3$	0
${}^3A_{1u}$												E_x

INTERACTION MATRIX

FIG. 3. Interaction matrix (see Refs. 7 and 12).

pure $^1P_1$ state. Under O_h symmetry the triply degenerate $^1T_{1u}\rangle_i$ states transform as the vector (x, y, z), which gives rise to the notation $|^1T_{1u}\rangle_x, |^1T_{1u}\rangle_y$, and $|^1T_{1u}\rangle_z$. Since the important basis functions here are spin-orbit mixtures of $|^1T_1\rangle$ and $|^3T_1\rangle$, the transition-probability matrix element becomes

$$\langle\Psi_f|\vec{r}|A_{1g}\rangle = [(1-t^2)^{1/2}\Gamma_{f,1} - t\Gamma_{f,9}]\langle^1T_{1ux}|x|A_{1g}\rangle\vec{i} + [(1-t^2)^{1/2}\Gamma_{f,2} - t\Gamma_{f,10}]\langle^1T_{1uy}|y|A_{1g}\rangle\vec{j} + [(1-t^2)^{1/2}\Gamma_{f,3} - t\Gamma_{f,11}]\langle^1T_{1uz}|z|A_{1g}\rangle\vec{k} \quad (6)$$

The corresponding oscillator strength is

$$f = (2m^*/3\hbar^2)h\nu|\langle\Psi_f|\vec{r}|\Psi_i\rangle|^2 . \quad (7)$$

Here $\Gamma_{f,j}$ represents the jth component of the twelve-component final-state wave function, t is the spin-orbit coupling term described above, and $x = x_1 + y_2$, $y = y_1 + y_2$, etc. Because of the symmetry and two-particle nature of the wave functions, each of the matrix elements appearing on the right-hand side of Eq. (6) reduces to[15]

$$I = \sqrt{\tfrac{2}{3}} \int R_s' R_s r^2\, dr \int R_p R_s r^3\, dr . \quad (8)$$

R_p and R_s' refer to the free-ion p and s radial functions associated with the $6s6p$ configuration, and R_s to the $6s^2$ configuration. Since we are concerned with relative values, the actual value of the radial integral is not important here.

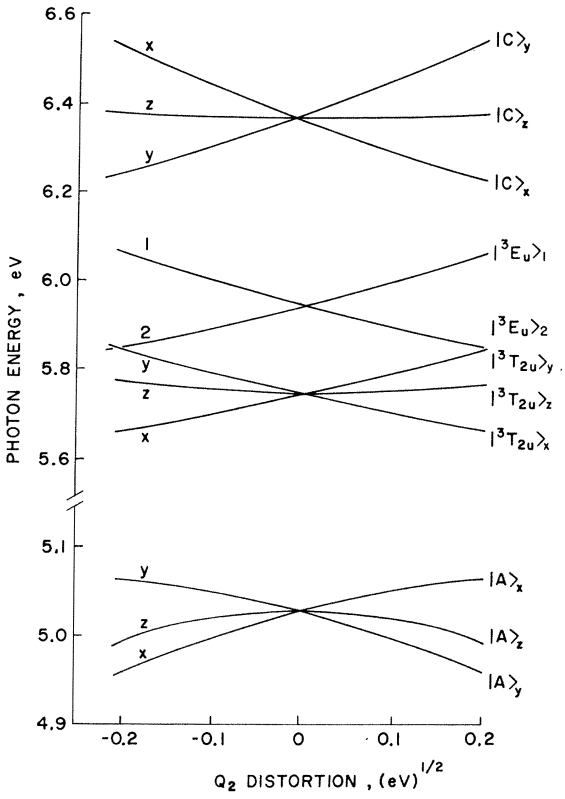

FIG. 4. Energy curves resulting from Q_2 distortion.

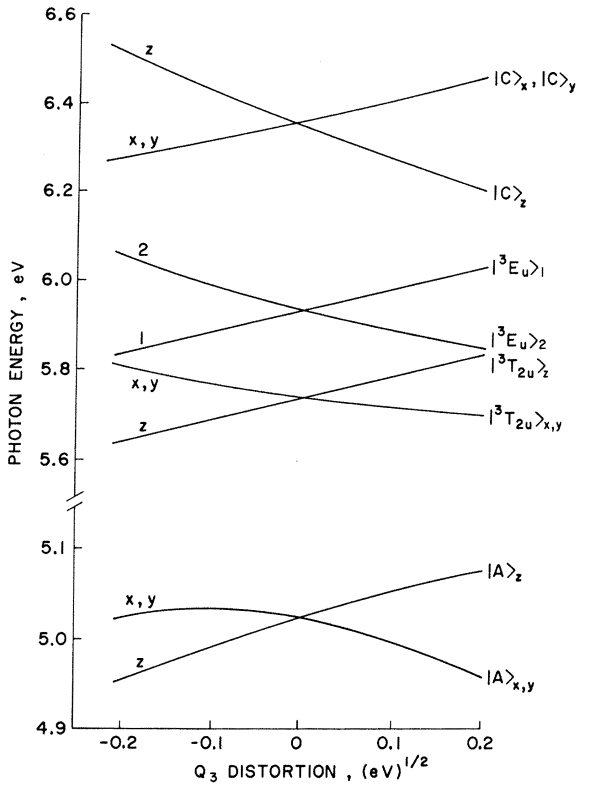

FIG. 5. Energy curves resulting from Q_3 distortion.

ENERGY-LEVEL SPLITTING AND BAND STRUCTURE

In general, the linear electron-lattice interaction results in a complete lifting of the degeneracy of the first excited state ($6s6p$). This lifting of the degeneracy is accompanied by a twelvefold mixing of the unperturbed excited-state wave functions. It is this mixing which gives rise to the B band and the lifting of degeneracy which gives rise to the triplet structure observed in the C and A Bands.[4,5] The lifting of degeneracies is most clearly seen by considering the effect which variations along one of the Q axes has on the energy splitting.

Energy Curves

Figures 4–6 show the results of the computer calculation as intersections of the five-dimensional energy surfaces with the various (Q, E) planes. On a physical basis it is not difficult to interpret these results. Consider, for example, the effect of Q_3 distortion (Fig. 7) on the C and A bands. Figure 7 shows the vibrational mode and the primary orbital form of the $|C\rangle_x$ and $|A\rangle_x$ states. It should be noted that the $|C\rangle_i$ states transform essentially as polar vectors, while the $|A\rangle_i$ states transform as axial vectors.[7] Because of the symmetry in the xy plane,

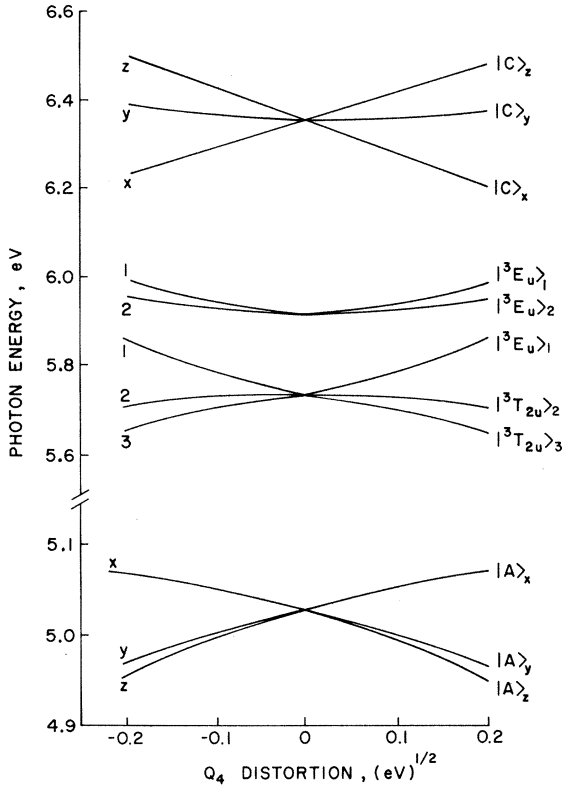

FIG. 6. Energy curves resulting from Q_4 distortion.

the energy variations of the $|C\rangle_x$ and $|C\rangle_y$ states should be identical and should be odd functions of Q_3. The effect of the Q_3 on the $|C\rangle_z$ state should be opposite to and more pronounced than that on the $|C\rangle_x$ and $|C\rangle_y$ states. This is because in the Q_3 mode the ions along the z axis vibrate out of phase and with larger amplitude than the ions located on the x and y axes.[16] In the case of the $|A\rangle$ states, the effect on $|A\rangle_x$ and $|A\rangle_y$ should be identical because of symmetry. Using the amplitude-phase argument above, the energy variations of these states should be opposite to that of the $|C\rangle_x$ and $|C\rangle_y$ states. The $|A\rangle_z$ state is affected principally

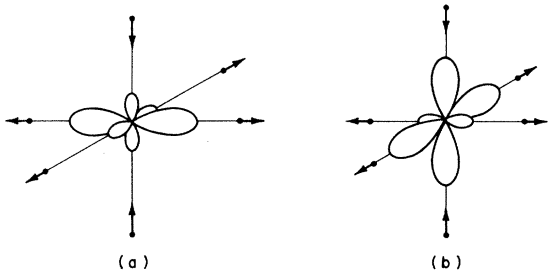

FIG. 7. (a) Interaction of Q_3 mode with $|C\rangle_x$ state; (b) interaction of Q_3 mode with $|A\rangle_x$ state.

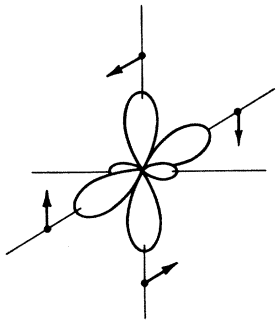

FIG. 8. Interaction of Q_5 mode with $|A\rangle_y$ state.

by the in-phase ion motion in the xy plane. Hence, its energy variation should be opposite and stronger than that of the $|A_x\rangle$ and $|A_y\rangle$ states. As in the case of the $|C\rangle$ states, the energy of the $|A\rangle$ states should be odd functions of Q_3. Figure 5 confirms this analysis.

Similar arguments concerning the effects of pure modes on any of the excited states yield the same type of qualitative agreement with the computed results. It should be noted that, in several instances, the energies are *even* functions of the distortion and that significant departure from linearity can be observed. This nonlinearity is due to the contribution from off-diagonal elements. A glance at Fig. 8, which shows the interaction between the Q_5-trigonal mode and the $|A\rangle_y$-state orbital, reveals immediately that the energies for this state are even functions of Q_5. If the oscillator strengths for these even energy states are not negligible, then *net* splitting should occur.

Oscillator Strengths

The oscillator strengths were determined by adding the oscillator-strength components of a given band. These *components*[17] followed the sense of the energy shifts in the Q space, increasing with increasing energy and decreasing with decreasing energy. The conclusion is that the band shapes should exhibit increased absorption toward the blue. Figure 9 shows the general behavior of the oscillator strengths of the A and C bands. Because this behavior was effectively the same for any coordinate Q or combination thereof, the abscissa in this figure is simply labeled as Q. It can be seen that the oscillator strengths are essentially constant over a wide range of Q. Only at extreme values does one notice a decrease in the C-band oscillator strength. The computed B-band oscillator strength shown in Fig. 10 is in sharp contrast to that of the A and C bands. It is strongly coordinate dependent and exhibits an almost exponential growth. The fact that C-band strength decreases at high Q values is not surprising in light of the extreme B-band

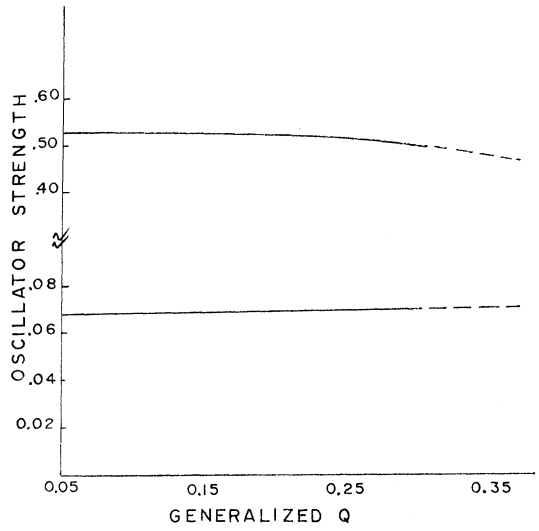

FIG. 9. C- and A-band oscillator strengths.

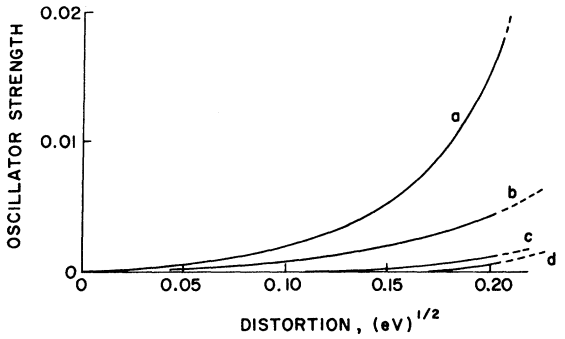

FIG. 10. B-band oscillator strengths; (a) $Q_4 = Q_5$; (b) Q_4; (c) $Q_2 = Q_3$; (d) Q_2 or Q_3.

growth. The meaning of the results is clear. Since Q is a measure of the temperature, varying roughly as $T^{1/2}$, the calculation reveals that (a) The A- and C-band oscillator strengths are almost temperature independent; (b) the B-band oscillator strength is strongly temperature dependent; (c) in the high-temperature region a decrease in the C-band oscillator strength should be observed; and (d) since the B-band oscillator strength is mode dependent, its strength should be affected by applied uniaxial stress.

Table I compares the oscillator-strength calculations with recent experimental results. Since an arbitrary value of 1.4 a.u. was used for the radial integral (see Ref. 15), no quantitative significance can be attached to the calculated results. Despite this, the table has several interesting features.

The computed C- and A-band oscillator strengths are consistently higher and lower, respectively, than the experimental results. This is because the value of the spin-orbit coupling parameter ($t = 0.37$) obtained by the KV procedure is too small. From Eqs. (3) and (7) it can be seen that the ratio of C- to A-band oscillator strengths varies as

$$(E_C/E_A)(1-t^2)/t^2 . \tag{9}$$

A value of $t = 0.40$ [18] yields the parenthesized results which compare favorably with experiment, indicating a stronger spin-orbit coupling than in the free ion.

The B-band results are clearly in disagreement with experiment and the increased spin-orbit coupling does not help. However, there are two important reasons for this disagreement. The first is that it is impossible to make an *a priori* unambiguous correspondence between Q value and temperature. In the case of the C and A bands this was unimportant since their oscillator strengths are almost constant over a wide range of Q values. On the other hand, the B band is strongly temperature dependent. This makes the correspondence essential for a determination of B-band oscillator strengths at different temperatures. The second reason is more subtle. Because of its strong temperature dependence, the B band is simply not Gaus-

TABLE I. Oscillator strengths, KCl:Tl.

Band	20 °K Calc	20 °K Expt (Ref. 5)	300 °K Calc	300 °K Expt (Ref. 5)	600 °K Calc	600 °K Expt
C	0.52 (0.50)[a]	0.48	0.52 (0.50)	0.47	0.508 (0.49)	...
A	0.066 (0.075)	0.077	0.067 (0.076)	0.075	0.068 (0.077)	...
B	0.001	0.005	0.007	0.032	0.17	...
C/A	7.9 (6.7)	6.3	7.7 (6.6)[a]	6.3	7.5 (6.4)	...
C/B	520	95	74	15	30	...

[a]Values in parentheses were obtained using a spin-orbit coupling parameter of 0.40 (Ref. 8).

sian or near-Gaussian at higher temperatures (~300 °K). Thus any experimental determination which assumes such a band shape is in error. Indeed, in our calculations it was found that at higher temperatures the upper E_g (B-band) levels actually merged with the lower C-band levels. This means that any subtraction technique used to separate the C and B bands at higher temperatures is certainly questionable. We are in the process of determining the shape of the B-band as a function of temperature. These results should resolve some of the difficulty.

SUMMARY AND CONCLUSIONS

A summary of the above computed results is that for each band there is *at least* one mode (a) for which the energy splittings (positive and negative) are even functions, and (b) for which the corresponding oscillator strengths are not negligible. From this the following conclusions may be reached: (i) *Net* temperature-dependent splitting of the A, B, and C bands does occur. This has been experimentally observed by a number of investigators, most recently by Fukuda[3] and Esser.[5] Figure 11 compares the experimentally analyzed splitting with that computed using only a Q_3 interaction. Despite this gross oversimplification there is reasonable agreement. Certainly a more complete analysis such as used by Cho[14] would improve the situation. (ii) In the case of the C band, a resolvable triplet structure is expected since the degeneracy of this state is completely removed under Q_3 for all temperatures. This has been experimentally observed.[3,19] (iii) For the A band, a doublet structure is expected at low temperatures where the degeneracy is not completely lifted. However, at higher temperatures (~300 °K), a triplet structure should be observed. This has been verified experimentally.[4,5,20] (iv) The B band should exhibit doublet structure since the computation reveals that only transitions to the two $|^3E_u\rangle$ states are nonnegligible. Recent analysis of the B band under uniaxial stress supports this prediction of a doublet structure.[21] At temperatures close to the melting point, the B band may exhibit more structure. However, we were not able to explore this possibility because of the intrinsic limitation of our perturbation scheme. (v) All of the bands should broaden with increased temperature. This is because of the instantaneous splitting and the fact that *net* splitting increases with increasing temperature. This has been observed.[3,5] (vi) The A- and C-band oscillator strengths should be almost constant over a wide range of temperature. This agrees with the experimental results.[5,22] However, at high temperatures close to the melting point, a definite decrease in C-band oscillator strengths should be observed. Patterson's work[4] indicates that this is the case. (vii) The B-band oscillator strength should be a rapidly increasing function of temperature. This has been observed experimentally.[3,5] (viii) The three bands should exhibit stronger absorption toward the blue. In the case of the A and C bands this seems to be the case as indicated by the asymmetry of the bands.[5,4] (ix) No transitions from the ground state to the $|^3A_{1u}\rangle$ state take place. This is because the transition probability to the $|^3A_{1u}$ state remained effectively zero throughout the range of Q values considered. This means that in an O_h environment, the $|^3A_{1u}$ state does not mix with the $|^1T_{1u}\rangle$ or with the $|^3T_{1u}\rangle$ state. On the basis of our model, we would *not* expect this state to contribute to the emission spectra unless an external stress were applied which would change the basic host symmetry.[20,23] No lower-energy absorption bands associated with Tl^+ have been observed.

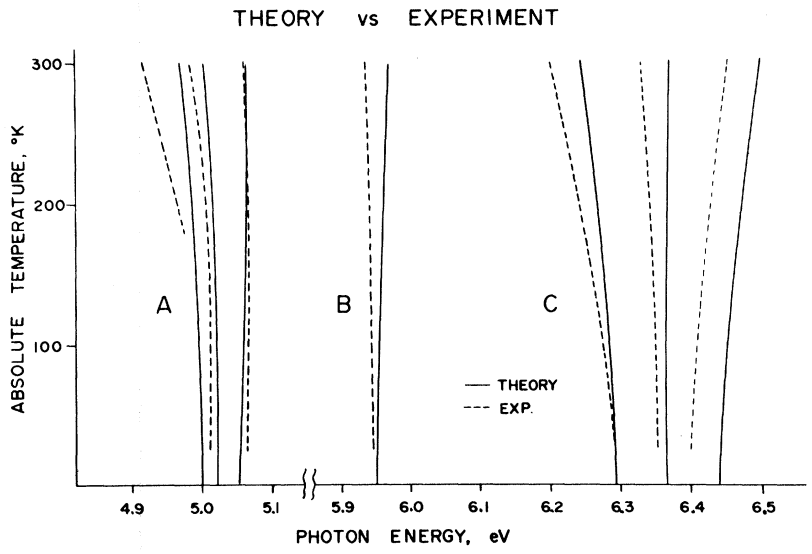

FIG. 11. Predicted absorption peaks using only trigonal distortion compared with experimental results (see Ref. 5).

In general, wherever contact can be made between experiment and theory, there is excellent qualitative agreement. This lends strong support to the model and method of attack we have used. The logical extensions of this problem, namely, the theoretical interpretation of the emission spectra, the effects of uniaxial stress on the absorption and emission spectra of KCl:Tl, and B-band shapes will be presented in subsequent papers. Furthermore, although the results were derived for KCl:Tl, the theory and general conclusions should be applicable to any heavy-metal ion such as Pb^{++}, In^{+}, etc., embedded in alkali-halide crystals.

ACKNOWLEDGMENTS

We would like to thank Dr. Paul Levy and Peter Esser of Brookhaven National Laboratory for keeping us abreast of their experimental results and for several interesting discussions. We would also like to thank Dr. Fred Williams for his fine pioneering efforts in the field and finally we wish to express our gratitude and admiration to the Japanese school for their excellent work which forms the basis for much of the material presented here.

---

*Present address: Research Department, Grumman Aerospace Corp., Bethpage, N. Y.

[1]F. E. Williams, J. Chem. Phys. 19, 457 (1951); Phys. Rev. 82, 281 (1951).

[2]F. Seitz, J. Chem. Phys. 6, 150 (1938).

[3]A. Fukuda, Sci. Light (Tokyo) 13, 64 (1964).

[4]D. A. Patterson, Phys. Rev. 119, 962 (1960).

[5]P. D. Esser and P. W. Levy, International Symposium on Color Centers in Alkali Halides, Rome, 1968 (unpublished); Bull. Am. Phys. Soc. 14, 325 (1969); (private communication).

[6]H. A. Jahn and E. Teller, Proc. Roy. Soc. (London) A161, 220 (1937).

[7]M. C. Stauber, Ph. D. thesis, Adelphi University, 1968 (unpublished).

[8]Y. Toyozawa and M. Inoue, J. Phys. Soc. Japan 21, 1663 (1966).

[9]G. W. King and J. H. Van Vleck, Phys. Rev. 56, 464 (1939).

[10]G. Herzberg, *Infrared and Raman Spectra* (Van Nostrand, Princeton, N.J., 1945), p. 122.

[11]H. Kamimura and S. Sugano, J. Phys. Soc. Japan 14, 1612 (1959).

[12]A. Honma, J. Phys. Soc. Japan 24, 1082 (1968).

[13]M. Tinkham, *Group Theory and Quantum Mechanics* (Interscience, New York, 1963), p. 67.

[14]K. Cho, J. Phys. Soc. Japan 25, 1372 (1968).

[15]In connection with other work, this integral has been evaluated using wave functions determined by both the Herman-Skillman and the Froese programs. The value is approximately 2.7 a.u. for the free Tl^{+} ion. R. Lucian (private communication); F. Herman and S. Skillman, *Atomic Structure Calculations* (Prentice Hall, Englewood Cliffs, N. J., 1963); C. F. Fischer, Computing Center, University of British Columbia, Vancouver, B. C., Canada, 1968 (unpublished).

[16]A. M. Lemos, and J. J. Markham, J. Phys. Chem. Solids 26, 1837 (1965).

[17]The only negligible oscillator strengths corresponded to transitions to the $^3T_{2u}$ (lower B-band) states and to the $^3A_{1u}$ state. This result is in disagreement with the conclusions reached by Bimberg *et al.* On the basis of absorption measurements made on a *stressed* crystal, they conclude that the B band is due to transitions to the $^3T_{2u}$ states. We find that if the local symmetry is changed from O_h to (say) D_{3d} ([111] stress), then indeed the B band is dominated by transitions to the $^3T_{2u}$ states. This is because by changing the symmetry, a certain trigonal mode is preferentially activated. However, under pure O_h this is simply not the case. D. Bimberg, W. Dultz, and K. Fussgaenger, Phys. Letters 25A, 766 (1967).

[18]The value of 0.40 is in fact the value empirically determined in Ref. 11.

[19]A. Fukuda, J. Phys. Soc. Japan 27, 96 (1969).

[20]V. Grasso and G. Saitta, Phys. Rev. Letters 22, 522 (1969).

[21]D. Bimberg, W. Dultz, and W. Gebhardt, Phys. Status Solidi 31, 661 (1969).

[22]W. Wagner, Physik 181, 143 (1964).

[23]J. Marion, Ph. D. thesis, Adelphi University, 1970 (unpublished).